Metrol. Meas. Syst., Vol. 28 (2021) No. 3, pp. 565–580
DOI: 10.24425/mms.2021.137136

PAN POLSKA AKADEMIA NAUK

METROLOGY AND MEASUREMENT SYSTEMS
Index 330930, ISSN 0860-8229
www.metrology.wat.edu.pl

M&MS

AN EVALUATION METHOD OF OBSERVABLE CHARGE TRAP DEPTH FOR THE PEA METHOD AND ITS COMPLEMENTARITY WITH THE Q(T) METHOD

Hanwen Ren[1)], Tatsuo Takada[2)], Yasuhiro Tanaka[2)], Qingmin Li[1)]

1) *North China Electric Power University, State Key Laboratory of Alternate Electrical Power System with Renewable Energy Sources, Beijing 102206, China* (*rhw112118@163.com*, ✉ *lqmeee@ncepu.edu.cn*, +86 01 061 772 304)
2) *Tokyo City University, 1-28-1 Tamazutsumi, Setagaya, Tokyo, 158-8557, Japan* (*takada@a03.itscom.net*, *ytanaka@tcu.ac.jp*)

Abstract

This paper proposes an evaluation method for the observable trap depth range of space charge when using the pulsed electro-acoustic (PEA) method and its complementarity with the current integration charge (Q(t)) method. Based on the measurement process of the PEA method and the hopping conduction principle of space charge, the relationship between the trap depth and the residence time of charge is analysed. A method to analyse the effect of the measurement speed and the spatial resolution of the PEA system on the observable trap depth is then proposed. Further results show when the single measurement time needs 1 s and the resolution is 10 μm at room temperature, the corresponding trap depth is larger than 0.68 eV. Meanwhile, under high temperature or with voltage applied, the depth can further increase. The combined measurement results of the PEA and Q(t) methods indicate that the former focuses on charge distribution in deep traps, which allows to calculate the distorted electric field. The latter can measure the changing process of the total charge involved in all traps, which is applicable to analysing the leakage current. Therefore, the evaluation of HVDC insulation properties based on the joint application of the two methods is more reliable.

Keywords: pulsed electro-acoustic method, trap depth, current integration charge method, leakage current.

1. Introduction

The accumulation of space charge in insulating materials is an important factor leading to severe distortions of internal electric field, development of partial discharge and appearance of electric tree, which is also a key characteristic for evaluating the aging and deterioration status of equipment insulation [1–3]. Generally, the insulation of an HVDC system withstands the joint effect of high voltage and high temperature which can cause a large amount of space charge accumulation [4, 5]. An accurate measurement and reasonable analysis of charge state in equipment insulation has thus become an important way to evaluate insulation properties effectively.

Article history: received February 23, 2021; revised May 14, 2021; accepted June 1, 2021; available online June 13, 2021.

After decades of rapid development, the mature measurement methods for charge-related characteristics currently comprise both types for measuring the charge distribution along the insulation thickness direction and ones for measuring the total charge amount through the insulation. The former mainly includes the *pulsed electro-acoustic* (PEA) method, thermal methods and pressure wave methods. Among them, the PEA method proposed by T. Takada [6], has been widely used in charge measurements in high-voltage DC and AC, high temperature and irradiation environments [7–10]. At the same time, the method is also developed to directly measure cables [11, 12], and recent studies have focused on signal distortion, optimal system design, and deconvolution algorithm for cable measurement [13–16]. The PEA method is mainly based on the pressure waves generated by space charge under the excitation with high-voltage pulses, which can be measured using a transducer to further obtain the charge information. In practical applications, the PEA method has two key features, *i.e.*, measurement speed and spatial resolution. Due to weakness of a single measurement signal, it usually needs multiple measurements for averaging to obtain a waveform with a high signal-to-noise ratio. Moreover, the spatial resolution of the method indicates that the results in this area can only display the total net charge [17]. However, the migration speed of space charge inside a sample depends on the trap depth [18, 19], and the trap depth of various materials depends, in turn, on their molecular structure [20, 21]. During the averaging process of multiple PEA measurements, the migration distance of the space charge in shallow traps may be very large, and, so far, its impact on the measured results has not been analyzed. The research on the effect of the measurement system performance from the perspective of the charge migration process will help to understand the trap depth range information when using the PEA method.

The current integration charge (Q(t)) method for measuring the total charge amount through the insulation was also proposed by T. Takada in 1972 [22]. The process of the total charge caused by surface-induced charge, absorption current and leakage current can be detected with this method, the reliability of which is also verified in comparison with the results of the PEA method [23]. Meanwhile, the Q(t) method can also be used for multi-layer materials, direct measurement of cables, IGBT modules and other devices in high-temperature environments [24–27]. It has the potential to be directly used for the equipment insulation since the measuring device can be connected to the high-voltage side for measurement. However, there is currently no analysis of the difference between the PEA and the Q(t) methods, and further discussion on joint application of the two measurement methods is also needed.

In the previous research work [3], the leakage current and conductivity calculation method of insulating materials based on the Q(t) method is proposed, which shows that the Q(t) method can measure the charge in shallow and deep traps. In this paper, the method of evaluation for observable charge trap depth in the PEA method is analyzed. The hopping conduction model is used to describe the space charge migration process, and an evaluation method for the relationship between the trap depth and the residence time of space charge is derived. The trap depth of accumulated charge that can be observed when using the PEA is then analyzed considering the system under the effect of measurement speed and spatial resolution. Further, the measurement results using the PEA and the Q(t) methods are studied, and the necessity of using the methods to jointly evaluate the insulation performance is discussed.

2. Measurement principles of the PEA and Q(t) methods

The measurement process of the PEA method is shown in Fig. 1. The space charge is injected and accumulates in the sample as a result of DC voltage applied. At the same time, high-frequency pulse voltages are applied to the sample with the accumulated charge, and the charge generates

Metrol. Meas. Syst., Vol. 28 (2021), No. 3, pp. 565–580
DOI: 10.24425/mms.2021.137136

pressure waves due to slight displacement of the charge layer. Then the pressure waves propagate towards the two electrodes. A piezoelectric transducer installed on the back of the grounded electrode converts the received pressure waves into a voltage signal which is amplified by an amplifier and finally recorded on a computer. Due to the time delay caused by the speed of acoustic waves when the signal propagates in the sample, the measured result can present the space charge distribution along the thickness direction of the sample [28].

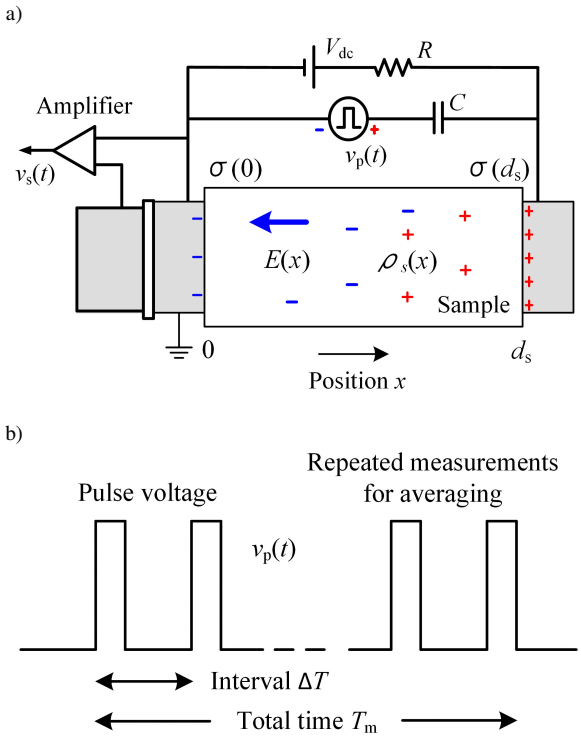

Fig. 1. Schematic diagram of the PEA system and measurement process. (a) PEA system, (b) measurement process.

The composition of pressure waves measured by the PEA system is shown in (1). $p(0,t)$ and $p(d_s,t)$ represent the two surface-induced charge signals of $\sigma(0)$ and $\sigma(d_s)$. $\Delta p(z,t)$ is the signal from the internal space charge $\rho_s(x)$.

$$p(t) = p(0,t) + \Sigma\Delta p(z,t) + p(d_s,t)\,. \tag{1}$$

In actual measurements, the measured voltage signal is very weak, *i.e.* only about a few microvolts before the amplification. Therefore, the measured single waveform using the PEA method usually contains a lot of random noise. It usually needs multiple-time measurements for averaging to improve the signal-to-noise ratio of the obtained waveform, as shown in Fig. 1b. When the frequency of pulse voltages is set as 1 kHz and 1000 measurement times for averaging are used, it takes 1 second to obtain a complete waveform. In addition, affected by the width of the pulse voltages and the thickness of the transducer, the spatial resolution of the system is usually at the micrometer level, and the final obtained results indicate the net charge within the resolution range.

When the space charge accumulates and migrates inside the sample under the applied DC voltage, the observed distribution is mainly affected by the characteristic of the charge trap depth in addition to the applied electric field. The migration process of charges affected by traps can be divided into the following two types in the PEA measurement:

1. The residence time of the charge at trap sites is longer than the single measurement time of the PEA system, or within a single measurement time, the migration distance of charge affected by the traps is shorter than the spatial resolution of the PEA system.
2. The single measurement time of the PEA system is longer than the residence time of the charge at trap sites, or within the measurement time, the migration distance of charge affected by the traps is longer than the spatial resolution of the PEA system.

The space charge distribution in the former state can be accurately measured using the PEA method. However, for the charge in the latter state, since it can make a long-distance movement before getting sufficient measurement times for averaging, the signal generated from this kind of charge is likely to be obscured by random noises at different locations. Therefore, it is difficult for the finally averaged waveform to show this part of charge distribution effectively.

Compared to the PEA method, the Q(t) method can measure all the charge information through the sample under the applied DC voltage [23, 24]. Its principle is shown in Fig. 2. The sample is surrounded by a three-electrode structure. Since the current $I(t)$ passing through the integrating capacitor C_{INT} and the high-voltage electrode in contact with the sample is the same, the total charge amount flowing through the sample can be obtained by integrating the current. The output of the high-voltage power source is automatically controlled by the computer, and the measured results are transmitted to it via a wireless transmission mode, *i.e.* with a ZigBee transmitter and receiver. The details of the measurement system were described elsewhere [23, 24].

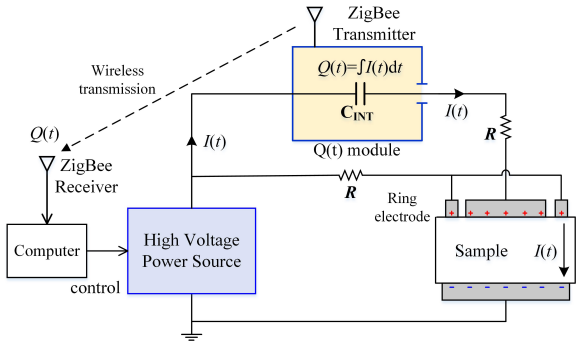

Fig. 2. Basic system of the Q(t) method.

From Fig. 3, it can be seen that after applying a DC voltage to the sample, the current flowing through the sample mainly contains three parts. Using the system in Fig. 2 to integrate the current, the corresponding Q(t) results also contain three parts, namely, initial induced charge amount Q_0, the space charge component $Q_{\mathrm{spac}}(t)$ and the leakage charge amount $Q_{\mathrm{leak}}(t)$, as shown in (2). The initial induced charge amount is equal to the product of the sample capacitance C_s and the applied voltage V_{dc}. $Q_{\mathrm{spac}}(t)$ and $Q_{\mathrm{leak}}(t)$ are the products of integration of the absorption current $I_{\mathrm{spac}}(t)$ and the leakage current $I_{\mathrm{leak}}(t)$, respectively.

$$\begin{aligned} Q(t) &= Q_0 + Q_{\mathrm{spac}}(t) + Q_{\mathrm{leak}}(t) \\ &= C_s V_{dc} + \int_0^t I_{\mathrm{spac}}(t)\,\mathrm{d}t + \int_0^t I_{\mathrm{leak}}(t)\,\mathrm{d}t\,. \end{aligned} \tag{2}$$

Metrol. Meas. Syst., Vol. 28 (2021), No. 3, pp. 565–580
DOI: 10.24425/mms.2021.137136

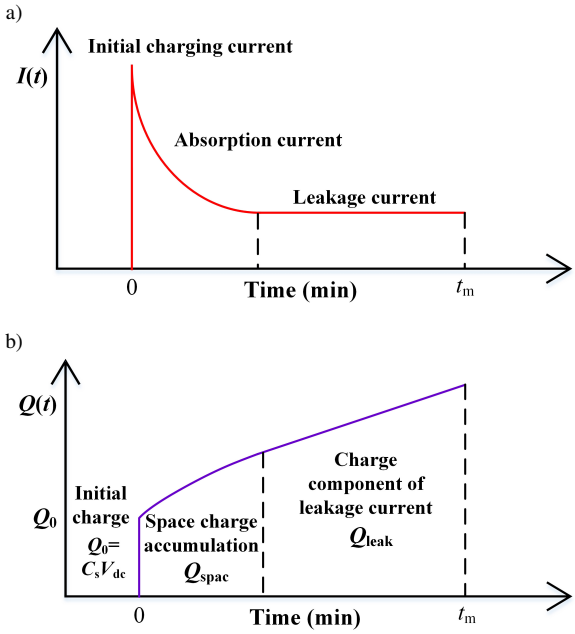

Fig. 3. The three charge components measured with the Q(t) method with a DC voltage applied. a) the current components, b) the corresponding charge components.

When establishing the Q(t) system, the effect of surface leakage current, integrating capacitor C_{INT} and protection resistor R should be considered. The ring electrode in Fig. 2 is used to reduce the effect of surface leakage current. Since high voltage is applied to the ring electrode and high voltage electrode, only a small surface leakage current is formed between these two electrodes which means that the measurement of Q(t) module connected to the high voltage electrode is not affected by this current.

The influence of integrating capacitance C_{INT} is discussed here. For the system in Fig. 2, when a high voltage V is output from the power source, the current flowing through the Q(t) module and the sample is the same, and thus the total charge amounts calculated by the current integration are the same. The charge amount Q can also be calculated by (3).

$$Q = C_s(V - V_{INT}) = C_{INT}V_{INT}\,, \tag{3}$$

where V_{INT} is the voltage withstood by the capacitor C_{INT}.

To sufficiently apply voltage V to the sample, it is required that V is much larger than V_{INT}. Thus, equation (4) can then be derived.

$$\frac{C_{INT}}{C_s} = \frac{V - V_{INT}}{V_{INT}} \cong \frac{V}{V_{INT}}\,. \tag{4}$$

Let us consider a film sample as an example. The polymer material with a thickness of 200 μm has a capacitance about C_s = 80 pF when the electrode area is about 8 cm^2. The maximum voltage that the Q(t) module can withstand is about 3 V. If the maximum voltage applied to the sample is V = 5 kV, the value of the capacitor should be about C_{INT} = 0.133 μF based on (4). We usually select C_{INT} = 0.15 μF for this situation. Thus, the ratio of C_{INT} to C_s is only about 0.05%.

It means that only a very small voltage proportion from the power source is applied to the Q(t) module. In addition, the performance of the Q(t) module was also tested for more than 12 hours. It is confirmed that the module can operate stably for a long time and its leakage charge is little. Therefore, the integrating capacitor C_{INT} has little effect in the method.

In addition, the protection resistor R in Fig. 2 is usually selected as 1 MΩ. Since the Q(t) method is used under DC voltages, the capacitive reactance of the sample is much bigger than this resistance. Thus, the protection resistor also has little effect on the measurement.

In the Q(t) measurement process, the induced charge is usually generated quickly at the beginning of the voltage application. Then space charge is injected into the sample and its distribution is gradually stabilized and, eventually, the absorption current tends to be zero. When the injected charge reaches the opposite electrode, the leakage current begins to appear and gradually reaches a stable value under the applied electric field. Since the Q(t) method measures all the current information from the beginning of the measurement after applying a high voltage, it can get all the charge information affected by deep and shallow traps.

Based on the criteria above for judging whether the PEA method is applicable to measuring the charge affected by traps, we propose an evaluation method for analyzing the trap depth range of the charge signal that can be observed using the PEA method. Then, we will discuss the effectiveness of the evaluation method of the joint use of the Q(t) and PEA methods on the charge accumulation characteristics in insulating materials.

3. The evaluation method for the observable trap depth range of the PEA method

3.1. The evaluation method based on the relationship between trap depth and residence time of space charge

The process of space charge hopping inside the sample affects its migration distance directly, and thus it can influence the observable information obtained with the PEA method according to the criteria above. Therefore, a hopping conduction model is used in this section to analyze the relationship between charge migration and sample trap depth [29], as shown in Fig. 4. In the figure, d_s is the sample thickness. T_d is the total time of charge hopping and trapping in the sample with traps. T_c means the hopping time of charge across the whole sample without traps. v and v_0 are the corresponding migration speeds of charge. N is the assumed number of traps in the sample. The distance between adjacent trap sites is c. The migration of an electron is used here as an example.

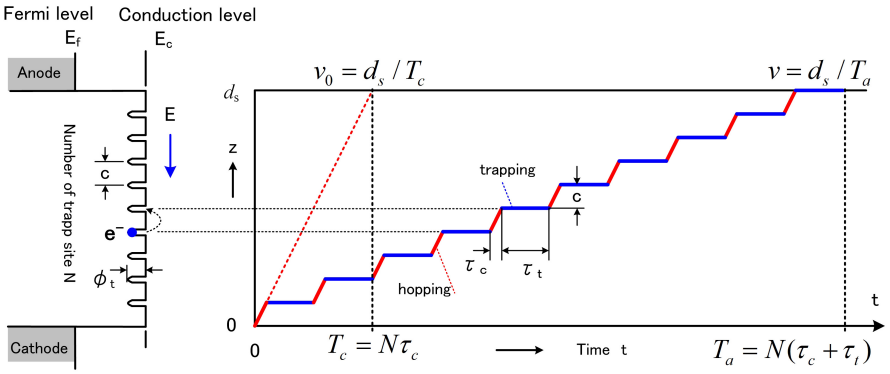

Fig. 4. Hopping conduction model of space charge inside the insulating material.

Metrol. Meas. Syst., Vol. 28 (2021), No. 3, pp. 565–580
DOI: 10.24425/mms.2021.137136

Under the effect of the electric field applied, the electron captured by a trap migrates toward the opposite electrode with a hopping probability θ_{hop}, which is determined by the residence time τ_t and the hopping time τ_c between adjacent trap sites, as shown in (5).

$$\theta_{\text{hop}} = \frac{\tau_c}{(\tau_c + \tau_t)} = \exp\left(-\frac{\phi_t}{kT}\right), \tag{5}$$

where ϕ_t, k and T represent the trap depth, the Boltzmann constant and the thermodynamic temperature, respectively.

Based on (5), the relationship between the residence time τ_t of charge and the trap depth ϕ_t can be further derived, as shown in (6).

$$(\tau_c + \tau_t) = \tau_c \exp\left(+\frac{\phi_t}{kT}\right). \tag{6}$$

The hopping time of electrons between trap sites can be estimated by the following derivation. The electron has both particle and wave properties. Its momentum p and energy E can be calculated using the following (7) and (8).

$$p = mv_e = \frac{h}{\lambda}, \tag{7}$$

$$E = \frac{1}{2}mv_e^2 = h\nu_0, \tag{8}$$

where m is the mass of an electron. v_e is its velocity. λ represents the wavelength of the electron wave. h is the Planck constant, and ν_0 is the vibration frequency.

In order to facilitate the estimation of the hopping distance of electrons, a linear model of polyethylene containing ketone functional groups as trap sites is taken as an example, as shown in Fig. 5. The electrons and holes distributed in polyethylene molecules are assumed to

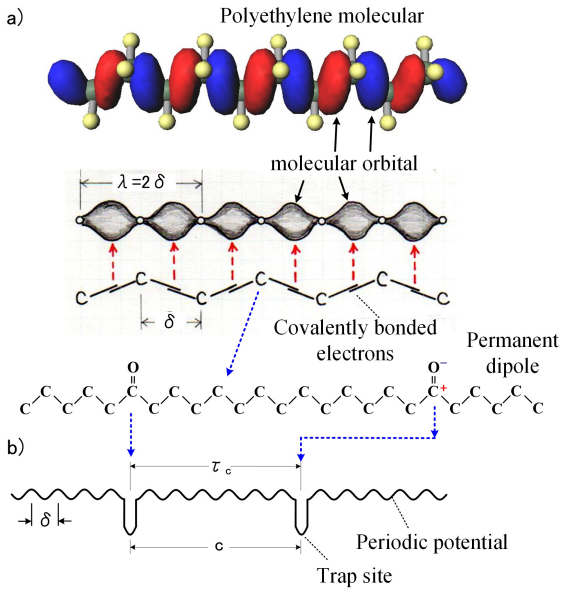

Fig. 5. Charge transport model controlled by trap sites. a) linear model of polyethylene, b) periodic potential between carbon atoms.

have the property of a one-dimensional stationary wave. It should be noted since various polymer materials can be used for electrical insulation, the calculation of the hopping distance c is expected to become a future research topic.

In the model shown in Fig. 5, the relationship between wavelength λ and spacing δ between the carbon atoms in the molecular chain is $\lambda = 2\delta$. A periodic potential distribution is formed between carbon atoms, and electrons can move under this electric field. When the vibration frequency at this time is v_0, its corresponding period τ_0 can be derived from (7) and (8), as shown in (9).

$$\tau_0 \left(= \frac{1}{v_0}\right) = \frac{2m}{h}\lambda^2 = \frac{8m}{h}\delta^2 . \tag{9}$$

Further, from Fig. 5b, it can be assumed that the hopping speed of the electron between the two trap sites is close to its movement speed in the molecule. The movement speed v_e can be derived from (7) and (8), and the relationship shown in (10) is then obtained.

$$\frac{c}{\tau_c} = \frac{2\lambda}{\tau_0} = v_e . \tag{10}$$

Based on (10), the relationship between the hopping time and the trap spacing can be obtained, as shown in (11).

$$\tau_c = \frac{2m\delta}{h}c . \tag{11}$$

For the polyethylene material, the atom spacing δ is 1.54 Å. With the mass of an electron and the Planck constant, the wave period in (9) can be calculated as 2.61×10^{-16} s. The vibration frequency can then be calculated as 3.84×10^{15} Hz. Therefore, the distance between trap sites determines the hopping time of the electron. The above derivation forms an evaluation method for the observable charge trap depth for the PEA method. The following evaluation will assume the distance between traps.

3.2. Evaluation of the Charge Trap Depth Range for the PEA method

Based on the evaluation method above and the obtained wave period, the change of trap depth under the effect of trap distance is analyzed. Fig. 6 shows the results of the trap depth with

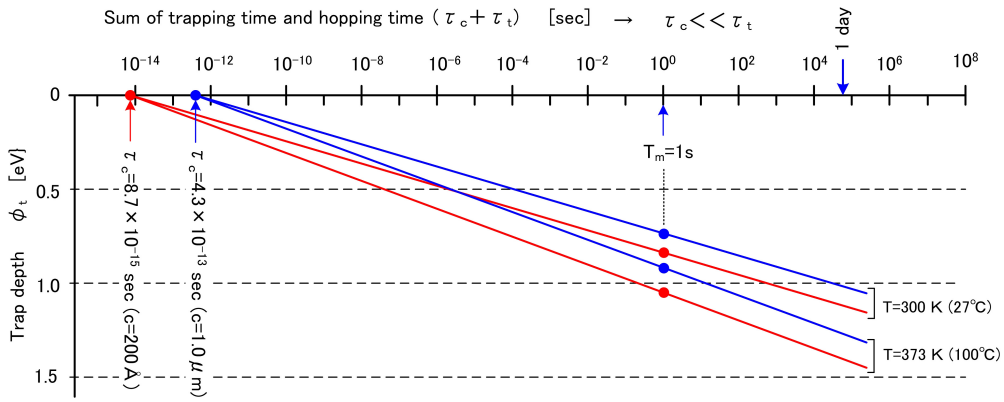

Fig. 6. Relation between the trap depth and the sum of hopping time and residence time.

Metrol. Meas. Syst., Vol. 28 (2021), No. 3, pp. 565–580
DOI: 10.24425/mms.2021.137136

different time calculated by (6). The abscissa of the figure indicates the sum of the residence time of the charge in a trap and the hopping time to the adjacent trap, and the ordinate indicates the trap depth. The curves under the two temperature conditions correspond to the two cases where the distances between the adjacent traps are 200 Å and 1.0 μm, respectively. If there are no traps in the sample, the residence time is zero. At this time, the lines in Fig. 6 intersect the abscissa axis, and the intercept is the hopping time. The selected trap depth in the figure is in the range of 0–1.5 eV. From the figure, it can be seen that within a large range of trap depth, the corresponding time is much longer than the hopping time. Therefore, the increase of residence time of charge mainly affects the change of the trap depth.

As stated in Section 2, one of the conditions for the PEA method to accurately measure the space charge is that "the single measurement time of the method is less than the residence time of the charge in the trap". When the measurement needs a large amount of averaging times, the criterion for the PEA method to observe the charge distribution accurately is the measurement time $T_m < (\tau_c + \tau_t)$. Since the hopping distance and time of charge residence are very short, it can be assumed that the residence time τ_t is the main influencing factor in the time axis. In addition, from Fig. 6, we can learn that temperature can also affect the range of the trap depth that can be observed using the PEA method. When the distances between the adjacent traps are determined, the condition at a higher temperature corresponds to a larger trap depth. It indicates that when measurement time T_m is determined, the corresponding measured space charge distributes in the trap range above a larger depth at a higher temperature.

let us now take the trap distance of $c = 200$ Å and the temperature of $T = 300$ K as an example, as shown in Fig. 7. The single measurement time of the PEA method is assumed to be 1 s and the resolution is 10 μm.

$$\frac{c}{\tau_c + \tau_t} > \frac{\Delta x}{T_\mathrm{m}}. \tag{12}$$

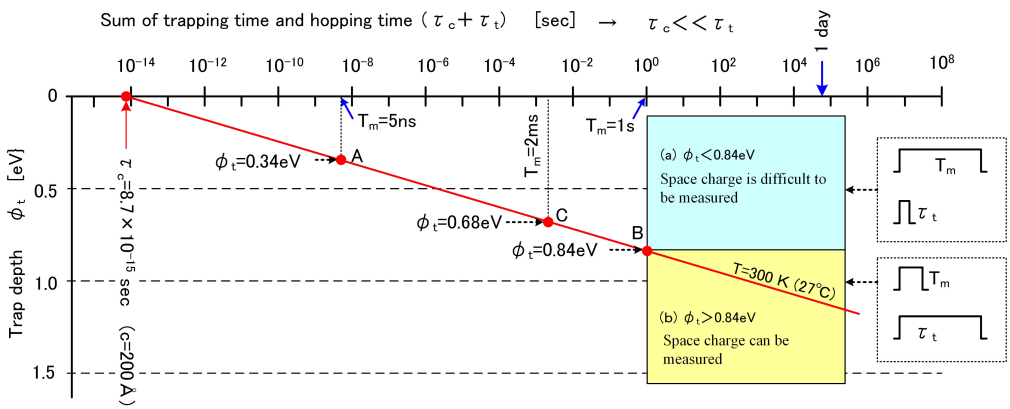

Fig. 7. Analysis of the measurement time and spatial resolution on observable trap depth.

Further analysis is shown below:

1. If there is an ideal PEA device, a signal with a high signal-to-noise ratio can be obtained under a single pulse excitation. If the pulse width for excitation is 5 ns, it can be seen from Fig. 7 that the trap depth corresponding to this time is 0.34 eV. Therefore, an ideal PEA device can detect the charge in a trap with a trap depth larger than 0.34 eV. However, in the actual measurement, the signal is obscured by the noise.

2. When a single measurement time is 1 s due to the measurement speed limited by the averaging process, Fig. 7 shows the trap depth is 0.84 eV. For the range of $T_m < \tau_t$ shown by the yellow area in Fig. 7, the PEA method can accurately measure the trapped charge in the trap depth larger than 0.84 eV. By contrast, for the part with the trap depth less than 0.84 eV, the charge can move a lot before the single complete measurement is completed. It is difficult to accurately measure the elastic waves generated by this part of the charge.
3. The relationship between the spatial resolution and the effectively measured signal: Set the pulse width is 5 ns, and the spatial resolution of the system is $\Delta x = 10$ μm. Let us consider the other condition described in Section 2 *i.e.* that the space charge distribution can be observed using the PEA system within the single measurement time, the migration distance of charge is less than the spatial resolution. Then equation (12) can be used to indicate the residence time of the observable charge using the PEA system.

This equation can be considered as that the migration speed of charge in adjacent traps is smaller than the speed threshold representing the ratio of the spatial resolution to the single measurement time. Combining with Fig. 7, the trap depth can be calculated as 0.68 eV. Therefore, this spatial resolution of the PEA system determines that it can only measure the trapped charge with the trap depth larger than 0.68 eV.

In addition, the detrapping probability of trapped charges actually changes with the increase of the applied electric field. The traps in polymer materials are caused by physical or chemical structures, *e.g.* traps are prone to generate at positions where polar groups exist or molecules are close to each other [20, 21]. Let us now consider a kind of rectangular trap with depth ϕ_t and width b, as shown in Fig. 8. When an electric field is applied to it, the trap depth decreases by $\Delta\phi(E)$ in the application direction, thereby easily releasing the trapped charge.

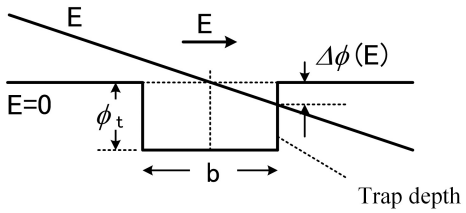

Fig. 8. Rectangular trap model.

Again, let us consider the effect of the applied electric field on the trap depth, as shown in (13). According to the size of the polar group in the polymer materials, the trap width is set to $b = 10$ Å. When the applied electric field is 10, 100, and 500 kV/mm, the trap depth can decrease by 0.01, 0.1 and 0.5 eV, respectively. Therefore, when the electric field is in the range of 100-500 kV/mm, the depth of insulation traps can decrease significantly. When combined with the results in Fig. 6, it becomes that the temperature condition can also affect the trap depth. Under high electric field and/or high temperature conditions, the information on space charge that can be observed by the PEA method will be reduced.

$$\Delta\phi(E) = \frac{b}{2}E\,. \tag{13}$$

Based on the discussion in this section, the spatial resolution and the single measurement time of the PEA system actually affect the trap depth range of the observable space charge captured in it. When the resolution is 10 μm with the measurement time of 1 s, these two conditions

correspond to the trap depth of 0.68 eV and 0.84 eV, respectively, *i.e.*, by using this PEA system, we can only obtain the charge information that is affected by the trap depth larger than 0.68 eV. Meanwhile, the temperature and applied electric field can also affect the range of the trap depth. The change of temperature is related to the time results calculated by (6), which has no effect on the spatial resolution part according to (12). The observable trap depth threshold should take the smaller of the two values calculated by the two equations.

3.3. Joint application of the PEA and Q(t) methods

Based on the conclusion analyzed above that the PEA method observes the charge information in the traps of deep depths, the PEA and Q(t) methods are used together here to analyze the charge performances of different materials when combined with the characteristic of the Q(t) method. Three gourps of measurement results under different samples are firstly selected, as shown in Fig. 9.

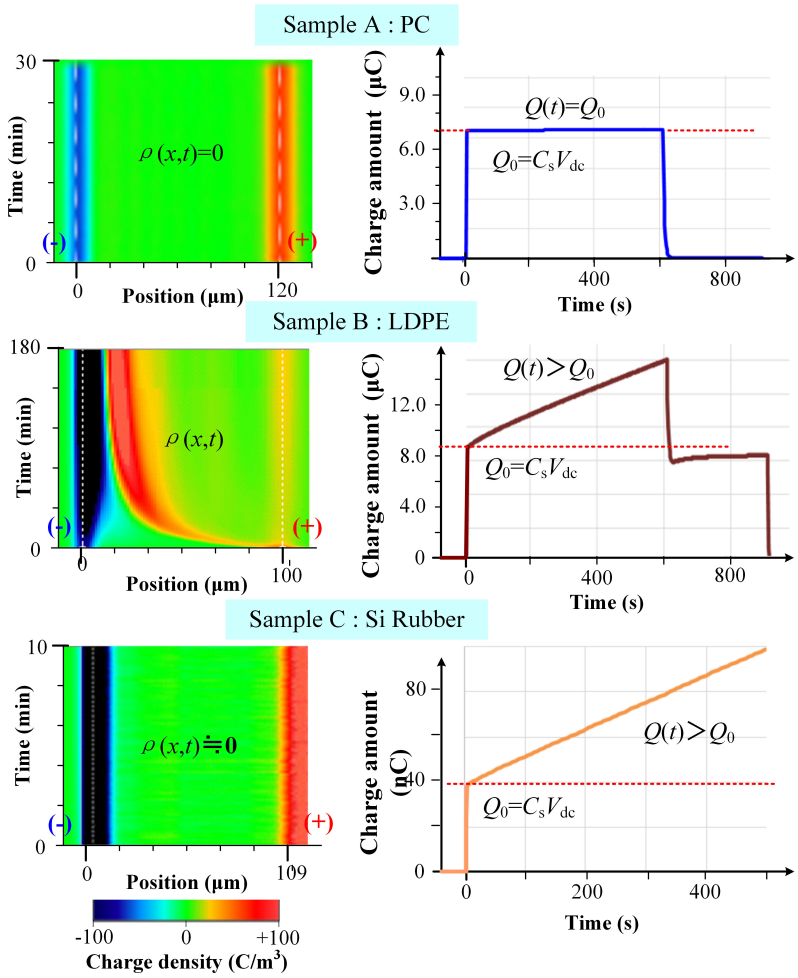

Fig. 9. Comparison between PEA data and Q(t) data [3]. Copyright Clearance Center's RightsLink® License Number: 5079690125049.

For the Sample A, the PEA results show that the amount of accumulated charge inside it is very small. At the same time, the charge amount flowing through it observed in the Q(t) data is basically equal to the initial induced charge amount which indicates that there are no charge accumulation and leakage current in it. By contrast, both the PEA and Q(t) results of Sample B indicate that the material cannot maintain good insulation properties under this measurement condition, and there are space charge accumulation and leakage current inside it.

However, the two methods differ in the evaluation for Sample C. From the PEA results, we can see that the accumulated charge is small, while the Q(t) data shows that the charge amount is increasing, which means that there is a large amount of charge accumulation and leakage current. When the two methods are used to analyze the insulation properties of the sample, opposite conclusions are obtained.

The charge amount measured with the two methods is further processed, as shown in Fig. 10. As stated in (2), the Q(t) data mainly contains three parts. The initially induced charge Q_0 is generated at the moment of voltage application, which is shown by the green part in Fig. 10. The integral result of the internal charge measured using the PEA method is shown by the red part in the Q(t) data.

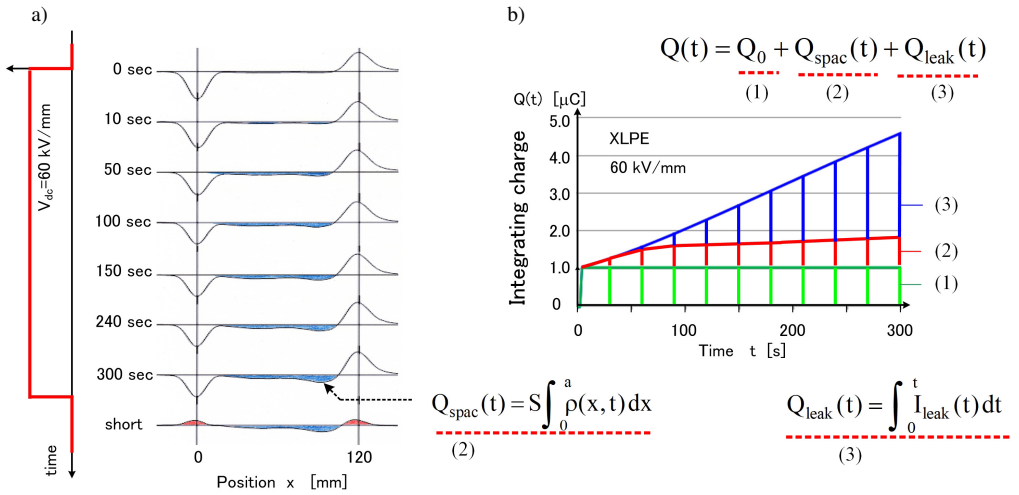

Fig. 10. Explanation of accumulated space charge $Q_{spac}(t)$ and leakage charge $Q_{leak}(t)$. a) PEA results, b) Q(t) results.

Let us consider the transition process from space charge accumulation to leakage current in the sample. When the measurement time reaches 300 s, the space charge distribution shown by the PEA results is basically stable. The charge in shallow traps that is difficult to detect by the PEA method gradually becomes the part of leakage current, and the Q(t) data continues to increase due to the existence of the large leakage current. After the leakage current stabilizes, the Q(t) result begins to increase linearly. At this time, a constant leakage current can be calculated from the increased slope $\Delta Q/\Delta t$.

Based on the analysis above, the PEA method can directly show the space charge distribution captured by deep traps, which can be further used to analyze the distorted electric field. By contrast, the Q(t) method mainly monitors the total amount of charge flowing through the sample, which makes it possible to analyze the characteristics such as leakage current under the effect of shallow traps. The Q(t) method can also be used to calculate material conductivity based on the measured leakage charge [3]. At the same time, previous experimental results have also accounted

for some joint use of the two methods. Similar with the results in Fig. 9, reference [23] finds that the total charge amount in PP material is much larger than that in PS material based on the Q(t) measurement, while the PEA results show the amounts of close accumulated space charge and distorted electric fields in both materials. The further analysis indicates that these phenomena are due to the charge with different polarities injected into the sample, which can be clearly shown by the PEA method. The research in [24] explores the space charge characteristics of double-layer samples. The results under DC voltages based on both methods indicate that space charge can be easily injected into an LDPE material in the LDPE/EPDM double-layer samples. However, under voltage polarity reversal conditions, the EPDM part shows a much more severe problem of charge accumulation in the case of the PEA method. In contrast, the Q(t) method still cannot be used under polarity reversal situation. In addition, reference [26] shows the advantage of the Q(t) method in direct evaluation of performances of the whole degraded cables as compared to the PEA method. Therefore, the two methods can present the different charge information on the measured material. It is recommended that both the PEA and Q(t) methods should be used to get the comprehensive information on induced surface charge, space charge accumulation, and leakage charge under the effect of deep and shallow traps.

4. Conclusions

According to the key performance of the PEA method and the hopping conduction model of space charge in insulation traps, the basic relationship between the trap depth and the residence time of charge in the trap is derived, based on which an evaluation method for observable charge trap depth is proposed. Theoretical analysis indicates that the measurement speed and the spatial resolution of the PEA system can determine the trap depth range of space charge that can be observed, which is also affected by temperature and applied voltage. When it takes 1 s to obtain a waveform after averaging with the spatial resolution of 10 μm, only the charges captured by traps with depths larer than 0.68 eV can be observed using the PEA system.

Combined with the comparative results of the PEA and Q(t) methods, it is further verified that the PEA method can only show the trapped charge distribution in deep traps inside the sample, while the Q(t) data reflect the change process of all charges flowing through the sample. When the charge distribution measured using the PEA method appears to be stable, the Q(t) data can be used to calculate the leakage current. The joint application of the PEA method for the research on distorted electric field distribution and the Q(t) method for the analysis on leakage current is necessary for the reliable evaluation of insulation properties.

In addition, the single measurement time and spatial resolution of the PEA method are set as constant values in this study. Meanwhile, the hopping time of the charge between adjacent traps is analyzed based on the example of the linear polyethylene chain. The researches related to polymer materials, such as the trap morphology depending on the structure of insulating molecules and the trap depth of various polymer materials which we can observe in the PEA measurement, still need further advancement.

Acknowledgements

This project was supported by the Beijing Natural Science Foundation (3202031) and the National Natural Science Foundation of China (Grant No. 51929701, 51737005, 52081330507).

References

[1] Zhai, J., Li, W., Zha, J., Cheng, Q., Bian, X., & Dang, Z. (2020). Space charge suppression of polyethylene induced by blending with ethylene-butyl acrylate copolymer. *CSEE Journal of Power and Energy Systems*, *6*(1), 152–159. https://doi.org/10.17775/CSEEJPES.2019.01150

[2] Wang, G., & Kil, G. (Sep. 2017). Measurement and analysis of partial discharge using an ultra-high frequency sensor for gas-insulated structures. *Metrology and Measurement Systems*, *24*(3), 515–524. https://doi.org/10.1515/mms-2017-0045

[3] Ren, H., Takada, T., Uehara, H., Iwata, S., & Li, Q. (Feb. 2021). Research on charge accumulation characteristics by PEA Method and Q(t) method. *IEEE Transactions on Instrumentation and Measurement*, *70*, 6004209. https://doi.org/10.1109/TIM.2021.3055288

[4] Dong, L., Gan, J., Zhang, P., Zhao, Z., Cheng, B., & Han, D. (2018). An improved resonant thermal converter based on micro-bridge resonator. *Metrology and Measurement Systems*, *25*(4), 715–725. https://doi.org/10.24425/mms.2018.124882

[5] Kuparowitz, M., Sedlakova, V., & Grmela, L. (2017). Leakage current degradation due to ion drift and diffusion in tantalum and niobium oxide capacitors. *Metrology and Measurement Systems*, *24*(2), 255–264. https://doi.org/10.1515/mms-2017-0034

[6] Takada, T., Maeno, T., & Kushibe, H. (1987). An electric stress-pulse technique for the measurement of charge in a plastic plate irradiated by an electron beam. *IEEE Transactions on Electrical Insulation*, *EI-22*(4), 497–502. https://doi.org/10.1109/TEI.1987.298914

[7] Gao, C., Qi, B., Gao, Y., Zhu, Z., & Li, C. (2019). Kerr electro-optic sensor for electric field in large-scale oil-pressboard insulation structure. *IEEE Transactions on Instrumentation and Measurement*, *68*(10), 3626–3634. https://doi.org/10.1109/TIM.2018.2881803

[8] Chen, G., Chong, Y., & Fu, M. (2006). Calibration of the pulsed electroacoustic technique in the presence of trapped charge. *Measurement Science and Technology*, *17*(7), 1974–1980. https://doi.org/10.1088/0957-0233/17/7/041

[9] Zhou, Y., Dai, C., & Huang, M. (2016). Space charge characteristics of oil-paper insulation in the electro-thermal aging process. *CSEE Journal of Power and Energy Systems*, *2*(2), 40–46. https://doi.org/10.17775/CSEEJPES.2016.00020

[10] Wu, J., Huang, R., Wan, J., Chen, Y., & Yin, Y. (2016). Phase identification for space charge measurement under periodic stress of an arbitrary waveform based on the Hilbert transform. *Measurement Science and Technology, 27*(4), 045004. https://doi.org/10.1088/0957-0233/27/4/045004

[11] Ghorbani, H., Abbasi, A., Jeroense, M., Gustafsson, A., & Saltzer, M. (2017). Electrical characterization of extruded DC cable insulation - the challenge of scaling. *IEEE Transactions on Dielectrical and Electrical Insulation*, *24*(3), 1465–1475. https://doi.org/10.1109/TDEI.2017.006124

[12] Mazzanti, G., Chen, G., Fothergill, J. C., Hozumi, N., Li, J., Marzinotto, M., Mauseth, F., Morshuis, P., Reed, C., & Tzimas, A. (2015). A protocol for space charge measurements in full-size HVDC extruded cables. *IEEE Transactions on Dielectrical and Electrical Insulation*, *22*(1), 21–34. https://doi.org/10.1109/TDEI.2014.004557

[13] Escurra, M. G., Mor, R. A., & Vaessen, P. (2020). Influence of the pulsed voltage connection on the electromagnetic distortion in full-size HVDC cable PEA measurements. *Sensors*, *20*(11), 3087. https://doi.org/10.3390/s20113087

[14] Imburgia, A., Romano, P., Chen, G., Rizzo, G., Sanseverino, R. E., Viola, F., & Ala, G. (2019). The industrial applicability of PEA space charge measurements for performance optimization of HVDC power cables. *Energies*, *12*(21), 4186. https://doi.org/10.3390/en12214186

[15] Rizzo, G., Romano, P., Imburgia, A., & Ala, G. (2019). Review of the PEA method for space charge measurements on HVDC cables and mini-cables. *Energies*, *12*(18), 3512. https://doi.org/10.3390/en12183512

[16] Jung, H., Kim, H., Choi, T., Hwangbo, S. (2019). Automatic measurement system of the space charge distribution by a two-step deconvolution. *Journal of Electrical Engineering and Technology*, *14*(5), 2049–2055. https://doi.org/10.1007/s42835-019-00169-y

[17] International Electrotechnical Commission. (2021). *Calibration of space charge measuring equipment based on the pulsed electro-acoustic (PEA) measurement principle* (Technical Specification No. IEC/TS 62758:2012). https://webstore.iec.ch/publication/7418

[18] Zhu, Y., Li, S., Min, D., Li, S., Cui, H., & Chen, G. (2018). Space charge modulated electrical breakdown of oil impregnated paper insulation subjected to AC-DC combined voltages. *Energies*, *11*, 1547. https://doi.org/10.3390/en11061547

[19] Tian, F., & Hou, C. (2018). A trap regulated space charge suppression model for LDPE based nanocomposites by simulation and experiment. *IEEE Transactions on Electrical Insulation*, *25*(6), 2169–2177. https://doi.org/10.1109/TDEI.2018.007282

[20] Li, J., Liang, H., Xiao, M., Du, B., & Takada, T. (2019). Mechanism of deep trap sites in epoxy/graphene nanocomposite using quantum chemical calculation. *IEEE Transactions on Electrical Insulation*, *26*(5), 1577–1580. https://doi.org/10.1109/TDEI.2019.008178

[21] Li, J., Zhao, R., Du, B., Su, J., Han, C., & Takada, T. (2020). Application progress of quantum chemical calculation in the field of HVDC insulation. *High Voltage Engineering*, *46*(3), 722–781. https://doi.org/10.13336/j.1003-6520.hve.20200331003

[22] Takada, T., Sakai, T., & Toriyama, Y. (1972). Estimation method of charge distribution in polymeric films. *IEEJ Transactions on Fundamental Materials*, *92*(12), 537–544. https://doi.org/10.1541/ieejfms1972.92.537

[23] Hanazawa, D., Sonoda, K., Miyake, H., Tanaka, Y., & Takada, T. (2018). Development of measurement system for DC integrated charge at high temperature. *2018 Condition Monitoring and Diagnosis (2018)*, Australia. https://doi.org/10.1109/CMD.2018.8535946

[24] Takada, T., Tohmine, T., Tanaka, Y., & Li, J. (2019). Space charge accumulation in double-layer dielectric systems-measurement methods and quantum chemical calculations. *IEEE Electrical Insulation Magazine*, *35*(3), 36–46. https://doi.org/10.1109/MEI.2019.8804333

[25] Sekiguchi, Y., Hosomizu, K., & Yamazaki, T. (2020). Conduction phenomena of AC- and DC-XLPE analyzed by Q(t) method. *2020 International Symposium on Electrical Insulating Materials (ISEIM)*, Japan, 166–168. https://ieeexplore.ieee.org/document/9275786

[26] Wang, W., Sonoda, K., Yoshida, S., Takada, T., Tanaka, Y., & Kurihara, T. (2018). Current integrated technique for insulation diagnosis of water-tree degraded cable. *IEEE Transactions on Dielectrical and Electrical Insulation*, *25*(1), 94–101. https://doi.org/10.1109/TDEI.2018.006738

[27] Fuji, M., Matsushita, K., Fukuma, M., & Mitsumoto, S. (2020). Study on characteristics of electrical tree in epoxy resin measured by current integrated charge method. *2020 International Symposium on Electrical Insulating Materials (ISEIM)*, Japan, 305–308. https://ieeexplore.ieee.org/document/9275799

[28] Fan, L., Tu, Y., Chen, B., Yi, C., Qin, S., Wang, S. (2020). Space charge behavior of polyimide at cryogenic temperatures. *IEEE Transactions on Dielectrical and Electrical Insulation*, *27*(3), 891–899. https://doi.org/10.1109/TDEI.2020.008704

[29] Li, J., Wang, Y., Ran, Z., Yao, H., Du, B., & Takada, T. (2020). Molecular structure modulated trap distribution and carrier migration in fluorinated epoxy resin. *Molecules*, *25*(3), 3071. https://doi.org/10.3390/molecules25133071

Hanwen Ren received his B.Sc. degree in electrical engineering and automation from North China Electric Power University, China in 2016. Currently he is a Ph.D. student at North China Electric Power University. From 2019 to 2020 he was a visiting researcher at Tokyo City University under the support of the China Scholarship Council. He is involved in research projects on space charge inside solid insulation and its measurement technology.

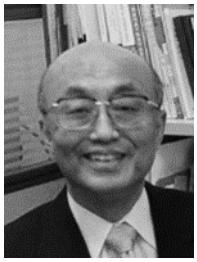

Tatsuo Takada received the B.E. degree in electrical engineering from Musashi Institute of Technology, Japan, in 1963 and the M.E. and the Ph.D. degrees from Tohoku University, Japan in 1966 and 1975, respectively. He became a Lecturer, Associate Professor and Professor at Musashi Institute of Technology, in 1967, 1974 and 1987, respectively. He was a Visiting Scientist at MIT (USA) from 1981 to 1983. He received the Excellent Paper Award from the IEE of Japan in 1974, 1981 and 1990. In 1990, he received the Whitehead Memorial Lectureship at the IEEE CEIDP. Currently, he is involved in several research projects on space charge effects in solid dielectric materials, surface charges on thin films, and electric field measurements in liquid materials.

Yasuhiro Tanaka received the B.E., M.E. and Ph.D. degrees in electrical engineering from Waseda University, Japan, in 1986, 1988 and 1991, respectively. He became a lecturer, Associate Professor and Professor at Musashi Institute of Technology, in 1992, 1998 and 2004, respectively. He was a Visiting Scientist at the University of Southampton from 1999 to 2000. Currently, he is conducting research and development work on the measurement system for space charge distribution in various solid dielectric materials at high temperatures under ultrahigh electric fields and spacecraft charge accumulation measurement in vacuum under electron-beam or gamma-ray irradiations.

Qingmin Li received his B.Sc., M.Sc., and Ph.D. degrees in electrical engineering from Tsinghua University, China, in 1991, 1994, and 1999, respectively. He joined Tsinghua University as a lecturer in 1996, and came to the UK in 2000 as a postdoctoral research fellow at Liverpool University and later at Strathclyde University. From 2003 to 2011, he was with Shandong University, China, as a professor in electrical engineering. In 2010 he also joined Arizona State University, USA, as a visiting professor. He is currently Professor of electrical engineering at North China Electric Power University, China. His special fields of interest include solid dielectrics, GIS/GIL insulation, lightning protection of wind turbines, condition monitoring and fault diagnostics.